Optical Materials 47 (2015) 566–572

Contents lists available at ScienceDirect

Optical Materials

journal homepage: www.elsevier.com/locate/optmat

Direct surface relief formation on As_2S_3–Se nanomultilayers in dependence on polarization states of recording beams

E. Achimova [a,*], A. Stronski [b], V. Abaskin [a], A. Meshalkin [a], A. Paiuk [b], A. Prisacar [a], P. Oleksenko [b], G. Triduh [a]

[a] Institute of Applied Physics of the Academy of Sciences of Moldova, 5 Academiei Str., 2028 Chisinau, Republic of Moldova
[b] V. Lashkaryov Institute of Semiconductor Physics NAS of Ukraine, 42 Nauki Ave., 03028 Kyiv, Ukraine

ARTICLE INFO

Article history:
Received 24 March 2015
Received in revised form 11 June 2015
Accepted 22 June 2015
Available online 25 June 2015

Keywords:
Diffraction gratings
Holography
Chalcogenide glass
Nanostructures
Polarization states

ABSTRACT

Direct one step grating relief formation by laser beam on the surface of amorphous chalcogenide nanomultilayers of the composition As_2S_3–Se was performed. Successive nanolayers on a glass substrate were prepared by thermal vacuum deposition with cyclic motion of substrate. Optical constants were obtained from transmission spectra data in the range of 450–900 nm. The dependence of the surface relief formation on nanomultilayers vs. the polarization states of laser beams was studied. The surface gratings with maximum relief depth were recorded under the two linear polarized beams falling on the sample surface at (+45°)–(−45°). Holographic diffraction gratings with the diffraction efficiency ~28% value in transmission mode at $\lambda = 0.65$ μm were recorded without additional treatment. This fact is explained by the contribution of mass transport whose direction is defined by the electric vector of laser beams. Recorded grating provides high optical quality of the obtained relief with depth of the grooves of about 100 nm at the total structure thickness 2500 nm.

1. Introduction

Over the past several decades, chalcogenide glasses (ChG) have attracted great attention due to their diverse range of optical and electrical properties, as well as due to a number of useful applications phenomena, induced in ChG by light having photon energy comparable to the bandgap [1–4]. It has been known that in ChG an exposure of a linearly polarized laser beam produces surface ripples, in which the rippling direction and periodicity seem to be governed, respectively, by the electric field and the wavelength of light [5]. Understandings of these photoinduced deformations are worth challenging, which may open a new scientific paradigm of light-matter interaction and applications to opto-deformable devices.

One of the fundamental physical phenomena used for producing various micro-optical elements on a surface of ChG films, such as surface relief gratings (SRG), linear waveguides and microlenses, is the photo-induced mass transport, which consists in lateral redistribution of amorphous material under illumination by the near-bandgap light [6–10]. Since these modifications are induced efficiently by illumination of the band gap light with photon energy of $h\nu \approx E_g$, where E_g is an optical gap of the material of interest, it is undoubtful that photoelectronic excitations activate successive electrostructural changes. However, it is difficult to identify the structural change, since the glass structure is disordered. In addition, in some phenomena, illumination of the linearly polarized light provides anisotropic changes, which are referred to as vectorial, which means that not only the photon energy value but also the direction of the optical fields vector exerts some influence on the photostructural processes.

Two main types of SRG induced by holographic recording, due to the excitation light modulation with near band-gap light in ChG can be distinguished according to their formation mechanism and their properties [11]:

1. Small scalar SRG induced by either volume expansion or shrinkage due to different response of the material in the bright and dark zones of the interference pattern formed.
2. Giant vectorial SRG induced by lateral mass transport in the case where the light polarization of the recording beams has a component along the light intensity gradient.

A number of studies have been carried out on photoinduced structural transformation in amorphous chalcogenides during the past few years, but here particular attention is given to the

* Corresponding author.
E-mail address: achimova@phys.asm.md (E. Achimova).

http://dx.doi.org/10.1016/j.optmat.2015.06.044
0925-3467/

polarization state of exposure light. In this report the direct (no wet development) surface relief formation during holographic recording in nanomultilayers (NML) As_2S_3–Se structure is presented. The influence of polarization states of recording beams on the stimulated structural changes which in turn can be used for surface relief shaping in NML As_2S_3–Se is studied in the work.

2. Material and methods

Although stimulated structural transformations were observed in a wide range of chalcogenide glass compositions, we selected for experiments As_2S_3–Se nanolayered films as well as Se and As_2S_3 layers because of their known parameters and well-known technology. Important criteria were low softening temperatures and low crystallization abilities of As_2S_3, small effects of the direct photostimulated scalar surface relief formation within the amorphous phase.

NML of ChG were prepared by computer controlled cyclic thermal vacuum successive deposition of bulk Se and As_2S_3 from two separated boats on continuously rotated glass substrate at room temperature in one vacuum deposition cycle [12]. The structural stability at interfaces and in the nanomonolayer is critical for any superlattice including NML. The direct determination of periodicity and roughness of interfaces of NML As_2S_3–Se deposited by the cyclic thermal evaporation was performed in [18] by Low Angle X-ray Diffraction where the author has shown the good quality of this NML. Deposition of the materials on the glass substrate was implemented through two separated windows. The technology allows a films deposition control within the whole sample thicknesses in the range from 0.005 up to 3.0 μm. The monitoring and determining of the total NML film thickness was carried out during the thermal evaporation by 2 interference thickness sensors at $\lambda = 0.95$ μm in transmission mode. The thickness of each nanomonolayer was calculated dividing the total measured thickness on a number of complete revolutions. In Fig. 1 the photograph (Fig. 1a) and the cross-section sketch (Fig. 1b) of the samples are shown. Overlapping part of the sample contains alternating nanolayers of Se and As_2S_3, i.e. two wide rings overlap in the central part of substrate forming NML As_2S_3–Se. The outside and the internal rings of layers on the substrate contain pure compositions of As_2S_3 and Se consequently. The layers of As_2S_3 and Se we obtained at the same time onto the same substrate consequently through the windows and used to check the composition, and calculate the ratio of the layer thicknesses in one modulation period N (the total thickness of one As_2S_3 and one Se nanolayers). As a result NML samples of As_2S_3–Se type structures with total thickness 1.5–2.5 μm and total number of nanolayers up to 100, the modulation periods $N = 10$–50 nm range, can be obtained.

To prevent the crystallization of Se layers, which are rather structurally unstable under heating and/or illumination, we minimized the heating of layers during the deposition by virtue of substrate rotation and reduced boat temperature.

The resulting samples were NML As_2S_3–Se structure with the total thickness 2500 nm and the composition modulation period $N = 25$ nm. The NML structure has a number of nanolayers of 100 + 100. Obtained films were investigated by an optical spectroscopy. Transmission spectra were measured in the region 450–900 nm with the use of spectrophotometer Specord M40 in order to determine separately the refractive index, the thickness and the optical band-gap energy of As_2S_3, Se layers and NML As_2S_3–Se.

An interferometric holographic recording was used to record a grating on the NML As_2S_3–Se like described in [13]. The period of the grating $d = \lambda/(2\sin\alpha)$, where λ is the wavelength of laser beam, α is the angle between the incidence laser beams. CW DPSS single mode laser operated at wavelength $\lambda = 532$ nm and average spot power density from 150 up to 350 mW/cm^2 on the sample was used for recording. The holographic gratings with a period of $\Lambda = 1$ μm were recorded by two symmetrical angled laser beams with respect to the sample surface normal. The intensity ratio 1:1 of the recording beams was used in order to achieve maximum interference fringes contrast. The phase shift experiments were performed by angular turning the quarter wave plates in each optical path, therefore, we can change the state of polarization of both recording beams. The two interfering beams independently pass through phase turning quarter wave plates to provide a control over the polarization state of the writing beams. Interfering beams with P–P, S–S, L–R or (+45°)–(−45°) polarization combinations were used for SRG recording.

The experimental set up is sketched in Fig. 2.

The diffraction efficiency η was controlled in real time by measuring the first order LD intensity in the transmission mode. The diffraction efficiency was determined as $\eta = I_{dif.}/I$ 100%, where I_{dif}–diffractive beam, I-transmitted beam in 0 order. During holographic recording all the changes in NML volume and surface (like those in absorption and refractive index) were controlled by measuring the transmission diffraction efficiency. Thus, the cumulative changes in diffraction efficiency η of NML As_2S_3–Se structure were measured.

3. Results and discussions

3.1. Optical properties

The transmission spectra of studied films are presented in Fig. 3. There is a broad transparency region at long wavelengths side and

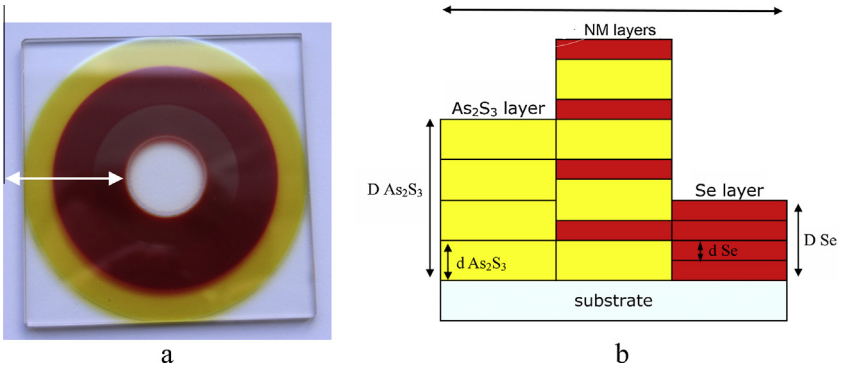

Fig. 1. (a) The photograph of NML As_2S_3–Se sample on polished glass substrate (75 × 75 mm^2) with the number of nanolayers 100 + 100. (b) Radial fragment of the cross-section of 4 As_2S_3 and 4 Se nanolayers formed of nanostructure on the substrate is shown (as an example). Horizontal arrows (in Fig. 1a and b) point to the same part of the sample. The vertical arrow indicates As_2S_3 and Se total thickness D_{As2S3} and D_{Se}, and the thicknesses of one layer d_{As2S3} and d_{Se}, consequently.